

# Advancements in the development of a proportional counter measuring system

Ondřej Kolář  
Department of Radio Electronics  
Brno University of Technology  
Brno, Czech Republic  
ORCID:0000-0003-4187-4890

Michal Kubíček  
Department of Radio Electronics  
Brno University of Technology  
Brno, Czech Republic  
ORCID:0000-0001-8247-8013

**Abstract**—This paper is an interim report of theory and continuous work on the proportional counter measuring system. The first part of the article covers general principles and properties of several types of electronic detectors for measuring the ionizing radiation fields including the proportional counters, to highlight their positives and negatives. The following part discusses the processing of proportional counter output signal. Next, the conducted measurement of a neutron source is described, and its results are shown. Based on the gained experience, the simulation and design of a new preamplifier for the measuring system was carried out.

**Index Terms**—ionizing radiation, proportional counters, measurement system, low noise amplifier, transimpedance amplifier

## I. INTRODUCTION

Ionizing radiation is utilized in many fields of modern science and research, but it is also used in power generation or commercially. It is a set of physical phenomena which can, by definition, ionize a material or medium that has been exposed to it. Depending on many factors, it can have potentially harmful effects on life organisms or inanimate objects. Therefore, the need for trustworthy and precise characterization of ionizing radiation fields is crucial.

The ionizing radiation can be described as a stream of moving particles. The number of particles traveling through a given area per unit of time is called particle flux, and it indicates the intensity of a given radiation field. The next important parameter is the energy carried by every individual particle since it indicates the amount of ionization that can be caused by the said particle. Last but not least, the type of particle is also very important. Based on all of these parameters combined, we can estimate the radiation behavior, its degree of danger, and also its source can be identified or studied.

## II. DETECTORS

Various detector types are used for the measurement of ionizing radiation. The choice of type depends on many factors and will vary for different applications. This article covers only some of the electronic detectors, but other types exist as well [1].

Research described in this paper was supported by the Internal Grant Agency of the Brno University of Technology under project no. FEKT-S-23-8191.

The most important aspect of every detector is its measurement capabilities. They differ in spectral and particle-type sensitivity and resolution, the maximum detectable intensity, or the output signal strength [2].

### A. Scintillation counters

Scintillators are a group of materials which emit visible light when irradiated with ionizing particles. Every incident particle transfers its energy to the material which then re-emits it in the form of a visible light impulse. These impulses are very short and dim, so for their conversion to an electric signal, photomultiplier tubes (PMTs) are often used [2]. The more energy the incident particle dissipates, the more photons of visible light are generated. This results in the output electric impulse being proportional to the energy of the originating particle. Thanks to this, scintillation counters are widely used for ionizing radiation spectrometry [2].

The scintillator could be of various materials [3]. Solid scintillators often come in the form of cylindrical crystals with a protective cover. Liquid scintillators must be contained in specialized sealed containers. Both of them must be made in such a way as to block all of the light from surrounding space, as any of it would overwhelm the scintillation photons and could potentially damage the PMT if turned on. They must also have an optical window for coupling with the PMT. This optical coupling has to be well-made to be as transparent as possible. The PMT serves two purposes. It transforms the optical signal into an electric signal, which then gets amplified for further processing in subsequent electronics [1] [2].

### B. Gaseous ionization detectors

Gaseous ionization detectors are a group of ionizing radiation detectors. All of them share the same general mechanical design, which is depicted in Fig. 1. Their electrically conductive shell is connected to the negative terminal of a voltage source. The positive terminal is connected to the anode, which usually consists of a thin wire in the center of the chamber. The inside of the chamber is filled with a gas or a gas mixture [2].

When an ionizing particle enters the detector, it ionizes the gas fill along its trajectory. The more energy the incident particle dissipates, the more of the gas gets ionized. These ions

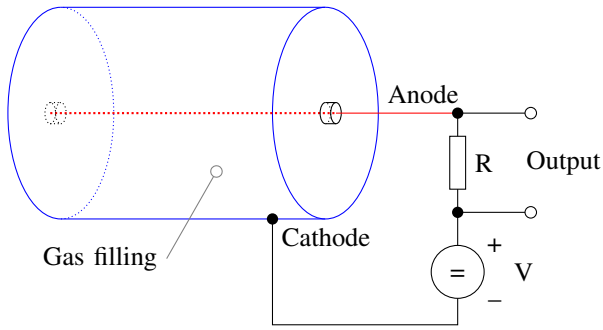


Fig. 1. Diagram of a simple cylindrical gaseous ionization detector [2]

start to move toward the corresponding electrodes as they are accelerated by the electric field. The acceleration is directly proportional to the intensity of the electric field, which is determined by the shape of both electrodes and the voltage supplied to them. When any ions finally reach the electrodes, they manifest as a current impulse at the output of the detector [2].

The optimal physical shape of the detector is chosen with respect to the intended region of operation, which then determines properties of the output signal. For a given detector shape, the region of operation depends on the supplied voltage as seen in Fig. 2. The chart shows the relation between the supply voltage and the output signal strength for two incident particles of different energies.

1) *Geiger-Müller tubes*: are a well-known group of gaseous ionization detectors designed to work in the region of operation of the same name. They are usually of a thinner cylindrical shape. Due to this, a high electric field intensity can be achieved without the need of a very high supply voltage. This strong electric field accelerates the primary free ions, created by an incident ionizing particle, so much that they hit other gas particles. This causes secondary ionization and causes a chain reaction that forms multiple Townsend avalanches

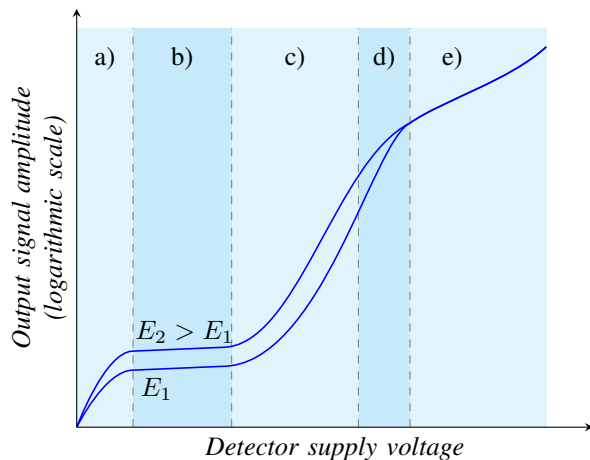


Fig. 2. Regions of operation of gaseous ionization detectors (a: ion recombination; b: ion saturation; c: proportional; d: limited proportionality; e: Geiger-Müller) [2]

throughout most of the detector interior. This means that the amplitude of the output current pulse is relatively high, therefore the subsequent processing of the signal is easy and does not require very sophisticated electronics. However, since the detector gas fill becomes saturated with the avalanches by any incident particle regardless of its properties, only the intensity of ionizing radiation fields can be measured with the Geiger-Müller tubes by counting the number of pulses per unit of time [2].

2) *Ionization chambers*: are a group of gaseous ionization detectors that work in the *ion saturation region*. On the contrary of the Geiger-Müller tubes, in this region, the primary ions are accelerated sufficiently so that neither their recombination is possible nor they could cause secondary ionization. This means that their amount is the same as the number of ions reaching the detector electrodes. Therefore, the resulting output current pulse is directly proportional to the energy dissipated by the incident ionizing particle. The downside is the small amplitude of such signal, so the requirements for a very high amplification and a low noise properties of the subsequent processing electronics are inevitable [2].

3) *Proportional counters*: are a group of detectors working in the *proportional region*, which combines the benefits of both previously mentioned regions. As the plot in Fig. 2 shows, the output signal amplitude remains proportional to the energy of an incident particle. Additionally, the amplitude also increases with higher detector supply voltages. This is caused by the electric field intensity near the anode in the detector center, which is higher than the minimum intensity needed for Townsend avalanche formation. The avalanche region is kept only within a small radius around the anode, as seen in Fig. 3, to ensure the formation of small nonoverlapping avalanches from primary electrons. This process multiplies the number of secondary ion pairs and is called *gas amplification* [2]. As the final number of ions is much larger, the output signal amplitude is higher, and so is the signal-to-noise ratio. Therefore, the low-noise requirements of processing electronics are less demanding than those of ionization chambers.

### III. PROPORTIONAL COUNTER SIGNAL PROCESSING

An output signal of a proportional counter comes directly in the form of an electric current pulse. Although its amplitude is higher, relative to an ionization chamber, it is still too weak for any direct processing. Therefore, it has to be amplified first. The specialized proportional counter preamplifiers often serve multiple purposes. In addition to amplification, they inject the supply voltage into the detector. They also transform the current signal to a voltage signal.

#### A. Particle energy measurement

Commercial preamplifiers for ionizing radiation spectrometry often come as charge sensitive amplifiers, which are basically integrating transimpedance amplifiers. Therefore, their amplification factor (gain) is given in units of mV/pC [4]. The integration of the signal comes with two benefits. The first is noise filtering, since the integrator behaves like

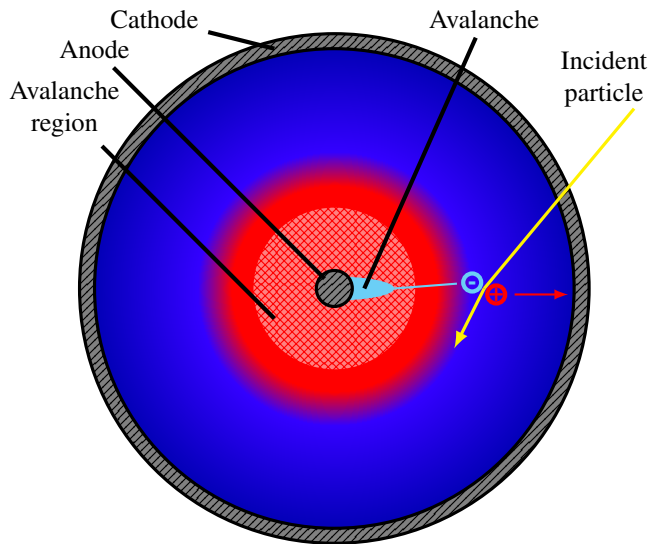


Fig. 3. Example of a single ion pair interaction in a cylindrical proportional counter [2] [5]

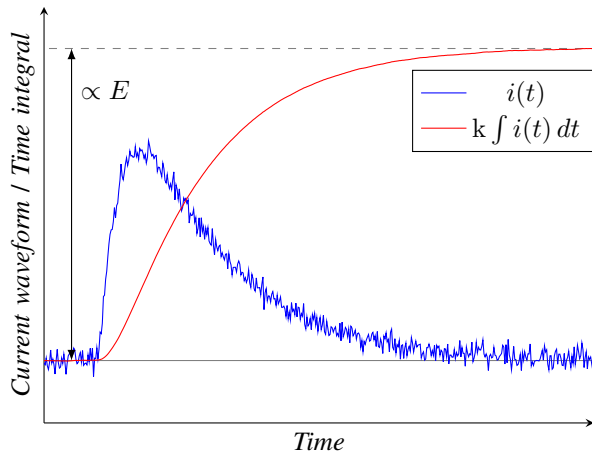


Fig. 4. Example of an artificial noisy current pulse and its numerical integration

a low-pass filter. The second benefit comes with the fact that the current  $i(t)$  through the detector terminals in any given moment is proportional to the rate of ions reaching the electrodes. By integrating this current pulse, it results in the total amount of charge generated by the incident particle which is proportional to the energy  $E$  dissipated by it. This simplifies further processing of the signal because the particle energy, which is of interest when using the proportional counter for spectroscopy, can be determined by measuring the height of the voltage step. To show both of these properties of charge sensitive preamplifiers, an example noisy pulse was generated and its integral (scaled by an appropriate constant  $k$ ) computed using MATLAB and plotted to Fig. 4.

### B. Pulse shape discrimination

When measuring ionizing radiation field, it can be composed of multiple types of particles simultaneously. One example of

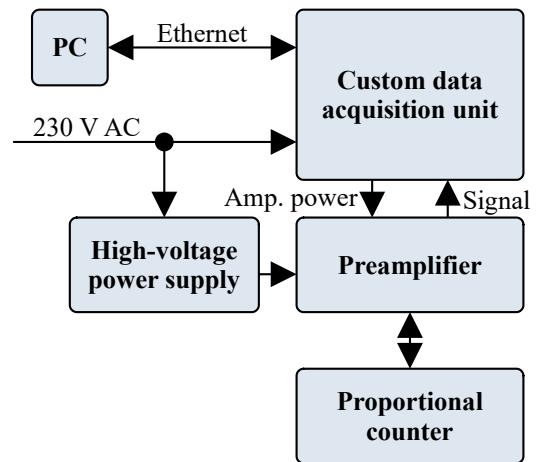


Fig. 5. Diagram of the measuring system

these mixed fields can be neutron radiation, which is often accompanied by gamma radiation, as the nuclear reactions usually produce both of them. For a proper characterization of such a field, the ability to separate them is important.

Pulse shape discrimination are various methods of signal analysis for classification of an incident particle type. For the scintillation counters, described in II-A, several of these methods are established and commonly used [6] [7]. However, the usual combination of charge sensitive preamplifiers and shaping amplifiers used with the proportional counters are deteriorating the original pulse shape. This makes them unusable for subsequent pulse shape analysis. The use of a non-integrating transimpedance amplifier is more suitable for the application of a pulse shape discrimination method [8].

## IV. MEASUREMENT

The custom developed measuring system used for data acquisition from proportional counters consists of several parts shown in Fig. 5. Its detailed description is covered in [9].

Using the system, the first real measurement of a radiation field was conducted at the Department of Electrical Power Engineering, FEEC, BUT. As a source of radiation the Americium-beryllium neutron source AS010/15, manufactured by Eckert & Ziegler Cesio s.r.o. was used. The commercial charge sensitive preamplifier used was the CSP10 manufactured by FAST ComTec GmbH. Its gain is  $1.4 \text{ V} \cdot \text{pC}^{-1}$ . The spherical proportional counter used for the measurement was manufactured by LND, Inc. with the serial number 270133 and it was supplied with 2500 V.

The detector was placed in the shielded room on top of a fixture in which the neutron source is securely kept. However, the number of detected events was too small to acquire a reasonable amount of data. To increase the number of detected particles, the neutron source was taken out of the fixture and placed at a distance of 20 cm from the detector. This drastically increased the number of detected events. A photo of the detector and source placement is in Fig. 6.



Fig. 6. Placement of the detector (left) and the neutron source (right) during the measurement

The measurement was run for 10 minutes and 5 seconds, during which the number of captured events was 15019. The average detection rate was approximately 24.8 events per second. The saved binary data was then loaded into MATLAB for processing.

Since the system saves the signal in raw form, a simple moving average filter was applied to filter out the noise first. The difference between the raw and the filtered signal can be seen in Fig. 7. The use of the integrating preamplifier facilitates easy computation of a measured energy spectrum by calculating the height of every impulse as described in Section III-A and plotting the values to a histogram (Fig. 8).

## V. PREAMPLIFIER DESIGN

Following the measurement, it was decided that a custom non-integrating amplifier for the measuring system will be designed and built. The reason for this is that the manufacturer prevents any modifications to the commercial CSP10, as the printed circuit board of the amplifier module is obfuscated by encasement in a black epoxy resin.

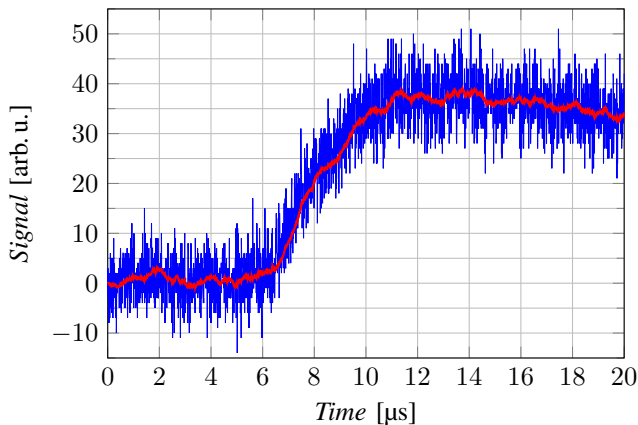


Fig. 7. Raw waveform of a captured event (blue) and its filtered form (red)

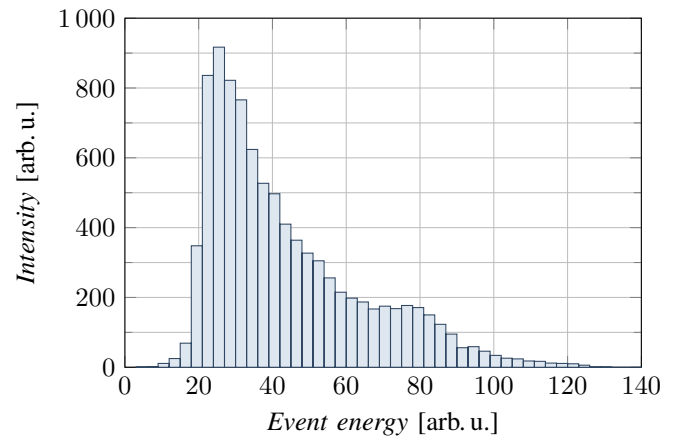


Fig. 8. The measured energy spectrum

As a core for the preamplifier, the AD8099 integrated circuit was chosen. It features an ultra-low noise operational amplifier with high-speed capabilities given by its gain-bandwidth product of 3.8 GHz [10]. The manufacturer Analog Devices, Inc. provides useful designer tools [11], including the Photodiode Circuit Design Wizard and SPICE model of the AD8099.

### A. First stage design

The Photodiode Circuit Design Wizard is an online tool for a simple and quick design of a photodiode transimpedance amplifier. The photodiode is simulated as a square waveform current source with its capacitance and shunt resistance in parallel. The values of all parameters can be set according to the required design. To model a proportional counter, the peak current was set at 100  $\mu\text{A}$  and the capacitance to 50 pF. The shunt resistance was set to 100 M $\Omega$  as this is a value of a resistor cascade through which the proportional counter is supplied with high voltage.

In the second tab of the tool, the AD8099 was selected. Various values of the required output signal parameters were then tried, and their influence on the estimated circuit characteristics was observed. The reasonable balance was found by setting the required bandwidth of 100 MHz, peak output voltage 100 mV, and peaking capacitor value 2.4 pF. The tool then estimated the output signal-to-noise ratio of 37.1 dB.

### B. Simulation

With the SPICE model of the AD8099 available, the circuit was transferred to the LTspice simulator. For better utilization of the maximum  $\pm 1\text{ V}$  range of the ADC in the acquisition unit, a second inverting amplifier stage with the voltage gain of 10 was added to the design. To ensure the modularity of the measuring system, both stages will be constructed separately, each of them in its own casing. This requires proper impedance matching to 50  $\Omega$  coaxial cables used for interconnection. The final simulation schematic is shown in Fig. 9. Running the noise analysis of the circuit in the range of 1 Hz to 1 GHz revealed its frequency characteristics, which are plotted in Fig. 10. The resulting bandwidth ranges approximately from

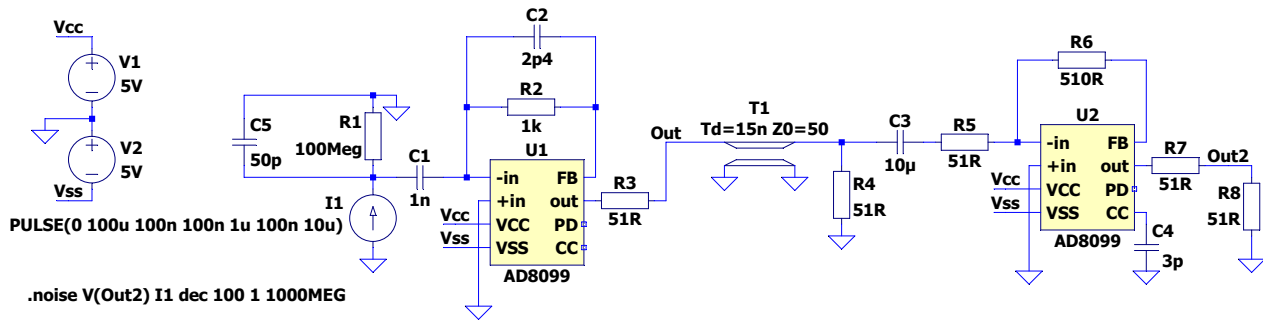


Fig. 9. The designed preamplifier simulation schematic

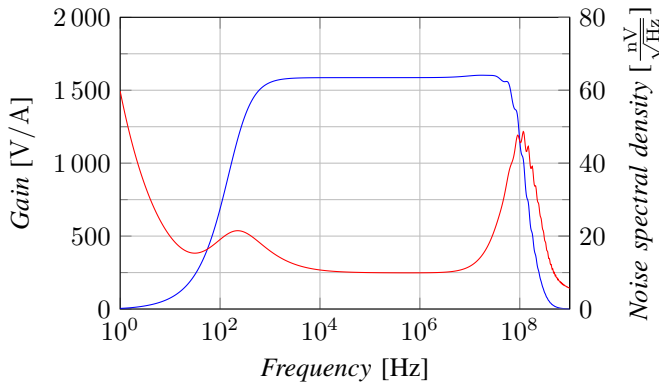


Fig. 10. The simulated frequency characteristics - gain (blue), noise spectral density (red)

246 Hz to 96.8 MHz with a gain of 1.59 V/mA. The total output RMS noise is 653.4  $\mu$ V.

### C. Physical design

The physical design of the preamplifier followed. To lower the cost of manufacturing, only a single universal version of a 4-layer printed circuit board (PCB) design was created using KiCad software. The board contains only one amplifier stage with all of the passive component footprints needed for populating either of the stages.

The power for the AD8099 amplifier is provided by the measuring unit which outputs a symmetric voltage of  $\pm 15$  V from its internal switching power supply. Since the voltage is quite noisy and too high for the amplifier, it is filtered by an LC filter and lowered to the  $\pm 5$  V by a dual symmetric low noise LDO regulator LT3032-5.

To ensure the low noise properties, the PCB was designed to fit inside an extruded aluminum enclosure, and on top of that, the AD8099 circuitry is placed under an additional SMT EMC shield to ensure suppression of any noise which could be brought inside of the amplifier enclosure with the power supply voltage.

## VI. CONCLUSION

Taking into account the theory and experience gained from the conducted measurement, a custom modular preamplifier

for the measuring system was designed. The design was verified using the LTspice simulator, which showed promising results. However, the simulation did not account for all real-world inaccuracies, such as parasitic parameters of the components used or especially the parasitic capacitance of the PCB, therefore the results might not be accurate and will need to be verified.

So, as a next step, a physical prototype of the preamplifier is about to be built, tested, and fine-tuned if necessary. At the time of writing this paper, the prototype is already in the process of production. The experimental results are therefore expected to be known soon.

## REFERENCES

- [1] V. Ullmann, "Detekce a spektrometrie ionizujícího záření", AstroNukl-Fyzika.cz.
- [2] G. F. Knoll, "Radiation Detection and Measurement," 3rd ed. Michigan: John Wiley & Sons, 2000.
- [3] B. D. Milbrath, A. J. Peurrung, M. Bliss, and W. J. Weber, "Radiation detector materials: An overview", *Journal of Materials Research*, vol. 23, no. 10, pp. 2561-2581, 2008.
- [4] FAST ComTec. (2023). *CSP10 Charge Sensitive Preamplifier* [Online]. Available: <https://www.fastcomtec.com/amp/csp10-charge-sens-preamp>
- [5] T. Neep, I. Katsioulas, P. Knights, J. Matthews, K. Nikolopoulos, and R. J. Ward, "A simulation framework for Spherical Proportional Counters", in *Proceedings of 40th International Conference on High Energy physics — PoS(ICHEP2020)*, 2021, p. 917.
- [6] G. Liu, M. D. Aspinall, X. Ma, and M. J. Joyce, "An investigation of the digital discrimination of neutrons and gamma rays with organic scintillation detectors using an artificial neural network", *Nucl. Instrum. Methods Phys. Res. A: Accel. Spectrom. Detect. Assoc. Equip.*, vol. 607, no. 3, pp. 620-628, 2009.
- [7] I. A. Pawełczak, S. A. Ouedraogo, A. M. Glenn, R. E. Wurtz, and L. F. Nakae, "Studies of neutron-pulse shape discrimination in EJ-309 liquid scintillator using charge integration method", *Nucl. Instrum. Methods Phys. Res. A: Accel. Spectrom. Detect. Assoc. Equip.*, vol. 711, pp. 21-26, 2013.
- [8] T. J. Langford, C. D. Bass, E. J. Beise, H. Breuer, D. K. Erwin, C. R. Heimbach, and J. S. Nico, "Event identification in 3He proportional counters using risetime discrimination", *Nucl. Instrum. Methods Phys. Res. A: Accel. Spectrom. Detect. Assoc. Equip.*, vol. 717, pp. 51-57, 2013.
- [9] O. Kolář, "Systém pro měření s proporcionálními detektory", Diplomová práce, Brno, 2022.
- [10] Analog Devices, "Ultralow Distortion, High Speed, 0.95 nV/Hz Voltage Noise Op Amp", AD8099 datasheet, 2016 [Rev. E].
- [11] Analog Devices. (2023). *AD8099 Tools & Simulations* [Online]. Available: <https://www.analog.com/en/products/ad8099.html#product-tools>